



# Active subglacial lakes beneath the stagnant trunk of Kamb Ice Stream: evidence of channelized subglacial flow

Byeong-Hoon Kim<sup>1</sup>, Choon-Ki Lee<sup>2\*</sup>, Ki-Weon Seo<sup>1</sup>, Won Sang Lee<sup>2,3</sup>, Ted Scambos<sup>4</sup>

- 5 <sup>1</sup>Department of Earth Science Education, Seoul National University, Seoul, 151-742, Republic of Korea  
<sup>2</sup>Department of Polar Geophysics, Division of Earth-System Sciences, Korea Polar Research Institute, Incheon 21990, Republic of Korea  
<sup>3</sup>Polar Sciences, Korea University of Science and Technology, Daejeon 34113, Republic of Korea  
<sup>4</sup>National Snow and Ice Data Center, University of Colorado, Boulder, Colorado 80309-0449, USA
- 10 *Correspondence to:* Choon-Ki Lee (cklee92@kopri.re.kr)

**Abstract.** We have identified two new subglacial lakes beneath the stagnated trunk of Kamb Ice Stream (KIS). Rapid fill-drain hydrologic events are inferred from Cryosat-2 altimetry, indicating that the lakes are connected by a drainage network. The orientation of the drainage network is inferred from the regional hydraulic potential, and clearly links the lake areas. The behavior of the subglacial lakes and strong thinning observed at the outlet near the grounding line implies that the subglacial water persistently flows from the region above the trunk to grounding line of KIS. In addition, the ice sheet in the KIS trunk estuary is thinning rapidly, and the thinning is accelerated by the activity of subglacial lake. We suggest that a transition from sheet flow of sub-glacial water to well-drained channelized flow may explain the shutdown of Kamb Ice Stream.

15

## 1 Introduction

Kamb Ice Stream (KIS), located on the eastern boundary of the Ross Ice Shelf, ceased rapid ice flow approximately 20 160 years ago (Retzlaff and Bentley, 1993). This stoppage is significant to understand the current mass balance of West Antarctic Ice Sheet (Pritchard et al., 2009). Catania et al. (2012) and Hulbe and Fahnestock (2007) indicated that Siple-coast Ice Streams have experienced stagnation and reactivation cycles, and the KIS is now in a stagnation phase of these cycles. Abrupt change in the basal hydrological system is a possible cause for the stagnation (Catania et al., 2006). van der Wel et al. (2013) also numerically showed that the long term velocity cycles of Kamb Ice Stream is associated with the basal melt and 25 upstream subglacial water supplies. Therefore, it has been suggestive that basal hydrology plays a critical role in the mass balance and dynamics of this region (KIS and the nearby Whillans, Bindschadler, and MacAyeal ice streams) and the Antarctic ice sheet as a whole (Bell, 2008). Understanding the region's subglacial hydrology and any evidence of its past evolution is critical to recover the history and predict its dynamics in this area (van der Wel et al., 2013). One hypothesis is that a change in the configuration of the subglacial drainage system from sheet to channelized water flow caused the 30 stagnation of the entire trunk of KIS (Retzlaff and Bentley, 1993), while no direct evidence of channelized flow beneath the KIS has been observed.



There are several subglacial lakes (SGLs) contributing the basal hydrology underneath the KIS (Figure 1). Although the existence of SGLs on KIS has been revealed by surface height variation from ICESat laser altimetry (Smith et al., 2009) and RADARSAT radar interferometry (Gray, 2005), little is known about the hydrological connection among adjacent lakes in KIS. Moreover, the ICESat repeat track method is limited by sparse coverage by the ground tracks, making it difficult to determine the lake boundaries in detail or to map small lakes. At present, the northern corner of KIS is morphologically understood as a margin lake due to thinning along the northern shear margin and retreat of the grounding line, similar to Subglacial Lake Engelhardt downstream of Whillans Ice Stream (WIS) (Fricker et al., 2007; Fried et al., 2014). A few simulations of present-day subglacial hydrology also suggest that a subglacial channel may still exist beneath KIS (Carter and Fricker, 2012; Goeller et al., 2015). However, none of the ICESat-based studies detected any signal associated with subglacial lake activity in the margin of the KIS trunk.

The Cryosat-2 radar altimeter launched in mid-2010 has provided topographic measurements of the Antarctic Ice Sheet with high spatial coverage and better elevation resolution than any previous radar altimeters. Owing to the dense ground track spacing of Cryosat-2, we discovered two unknown subglacial lakes. Activity on the lakes appears to have been triggered by sequential filling events in upstream lakes. The sequential activities from upstream subglacial reservoirs to the trunk hydrologic system of KIS provides critical evidences on the characteristics of the basal environment under the trunk of KIS.

## 2 SGL Detection from Cryosat-2 Measurements

The Cryosat-2 operates three different modes, Low Resolution Mode (LRM), Synthetic Aperture Radar (SAR), and SAR interferometric (SARin) (Wingham et al., 2006a). The SARin mode provides a determination of the precise reflecting (backscattering) point on the surface. A nominal spatial resolution of this mode of measurement is ~300 m and ~1km for along- and across-track directions, respectively (Wingham et al., 2006a). The geophysical mask of SARin mode covers the margins of the ice sheets or the mountainous regions with higher slope than the ocean or ice sheet interior. We primarily utilize the Level 2 (L2) product of SARin mode, which directly provides geospatially corrected surface elevations with various correction terms and error flags. The vertical accuracy of SARin mode ranges from 0.17 m to 0.65 m on the interior of ice, although the magnitude of the surface height error highly depends on the slope of the imaged surface (Wang et al., 2015).

To detect SGL in the study area, we adopt the similar data processing used in McMillan et al. (2014). In order to remove the low quality returns of L2 products, we first remove outliers with the height error flags or extremely high backscatter values (>30dB) and then recursively apply a 3-sigma filter to the elevation residuals deviated from a recent DEM product (Helm et al., 2014). To estimate an elevation change rate in a 5 by 5 km region, a quadratic curved surface fitting the Cryosat-2 elevation measurements in the whole time period (July 2010 – February 2015) is determined and used for removing the topographic undulation in detail from the elevation measurements. From the topography-free elevation



residuals, we finally estimate the linear elevation change rate within a two-year time window and successively shift the time window with a 3-months interval. To increase the spatial resolution, 5 by 5 km regions for elevation change rate are overlapped with 1 km spacing. Using the resulting successive maps of elevation change rate, we visually inspect the spatiotemporal variation of elevation change rate and detect candidates of subglacial lake. For example, Figure 2 shows the elevation change rate and its uncertainty (regression error) from February 2012 to January 2014 in the trunk of KIS. We can identify two new active subglacial lakes as shown in red boxes because their uncertainties are sufficiently lower than those on other anomalous regions. Moreover, they are located on a ‘potential subglacial lake’ area identified from previous analysis of continent-wide sub-glacial hydropotential (Livingstone et al., 2013). We named the lakes as Kamb Trunk 2 (KT2) and 3 (KT3), because they seem to be activated by an upstream lake Kamb Trunk 1 (KT1) already identified by ICESat (Smith et al., 2009).

In order to specify a more detailed boundary of the KT2 and KT3 SGLs, we first generate a reference digital elevation model (DEM) from the Cryosat-2 elevations during July 2010 – December 2011 using a kriging method (Goovaert, 1997) (Figure 3a). The reference DEM is compared to the other DEMs in various time windows in order to find a clear elevation change. The time windows of May 2013 - January 2015 for KT1 and July 2013 – January 2014 for KT2 and KT3 yield the clearest elevation anomaly indicating SGL boundary (Figure 3b). A contour line with the same value as the standard deviation of the background elevation anomalies (i.e. elevation anomalies in the region adjacent to the SGL) is empirically chosen as the lake boundary, since it makes a good agreement with the lake boundary independently inferred from the repeat track analysis of ICESat measurements for KT1. As a result, the area of KT1, KT2, and KT3 are 43.5, 31.7 and 38.7 km<sup>2</sup> respectively. The hydraulic potential surface derived using the reference DEM and the ice thickness of BEDMAP2 (Fretwell et al., 2013) strongly supports the existence of two new SGLs as well as lake KT1 (Figure 3c).

### 3 Result and Interpretation

#### 3.1 Hydrological connectivity of subglacial lakes in the Kamb Ice Stream

Understanding the characteristics of the hydrologic connection between the SGLs will contribute greatly to development of a conceptual model of the present sub-glacial water system. We investigate the temporal changes of newly discovered SGLs and the known KIS SGLs to understand their hydrological connectivity. After removing the reference DEM elevations from the Cryosat-2 measurements, the residuals within the lake boundary are averaged in the interval of a month to generate the time series of elevation change. The background temporal elevation changes outside the lake boundaries are removed to examine only the elevation changes associated with the SGLs activity. The volume change is calculated by simply multiplying the elevation change and the area of lake. Figure 4 shows the elevation and volume changes of three SGLs, representing the sequential filling events in 2013. The volume of lake KT1 begins to increase in early 2013. Roughly two months later, the volume of lake KT2 starts to increase, and about another two months later, the volume increase of lake KT3 also begins. The volume of lake KT1 is increased by ~ 0.1 km<sup>3</sup> during ~6 months, which indicates the



balance flow rate of inflow and outflow is  $\sim 6 \text{ m}^3/\text{s}$ , roughly. The sudden volume increase of lakes KT2 and KT3 also show similar filling rates. Sequential drops in lake volume after the filling events are also observed but in an opposite order. The excess water in lake KT3 was completely drained in 8 months after the start of filling event, whereas the Lake KT2 returned to the previous volume level in 16 months, and the volume of KT1 did not descend completely yet.

5 It is interesting to note that the volumes of downstream lakes KT2 and KT3 begin to increase before the upstream lakes are entirely filled. Another important observation is that there is no volume change in lake KT3 during the drainage stage of KT2 in the middle of 2014. These two facts may imply significant hydrological characteristics of the lake system. Wingham et al. (2006b) have reported that three lakes along a line of  $\sim 100 \text{ km}$  in the Adventure Trench Region experienced simultaneous fillings by the water supply from an upstream lake. To explain this behavior, Carter et al. (2009) suggested that  
10 the high variability of local water pressure in the turbulent water flow is more significant than a few meters of hydraulic head difference as a barrier between adjacent lakes. Similarly, Fricker and Scambos (2009) have observed a linked drainage event between Subglacial Lake Conway and Subglacial Lake Mercer in the Whillans and Mercer ice streams, but the volume changes of the two lakes are not always explained by a direct relationship between the drainage from upstream and filling of  
15 downstream reservoirs. They explained that the opening of an outlet conduit for the downstream lake allows the additional floodwater from the upstream lake to move directly through the downstream lake without increasing its water level. Therefore, we can suggest that the three lakes in the trunk of Kamb Ice Stream are closely connected by conduits that are easily opened by turbulent water flow. As shown in Figure 3c, the hydraulic potentials at the outlet (inferred along the  
20 streamline) of lakes KT1, KT2, and KT3 are 30 – 80 kPa higher than the minima inside the lakes. The potential differences are equivalent to the head differences of 3 – 8 m, roughly consistent with the maximum elevation changes inside the lakes when the lakes are fully filled. Therefore, to account the early fillings of downstream lakes, the lake water should flow over the hydraulic barriers through the conduits before the hydraulic head reaches the full capacity of lake. The direct pass through the lake KT3 of the drained water from KT2 in the middle of 2014 also suggests the opening or growth of conduit caused by flood events could diminish the role of hydraulic barrier.

The three SGLs in the trunk of KIS appear to be connected with SGLs in the region upstream of the KIS trunk  
25 where the ice stream is still flowing, according to the model study of Goeller et al. (2015). Cryosat-2 measurements are also used to find the source of the flood event. The geographical mask of Cryosat-2 SARin mode, unfortunately, does not cover the upstream KIS area but the LRM mode, which has relatively poorer spatial resolution than SARin mode, is available over the area. Using the LRM mode products, we detected large elevation changes in three lakes, Kamb 1 (K1), Kamb 3-4 (K34), and Kamb 8 (K8), upstream of KIS. Other upstream lakes in the KIS trunk do not show any apparent elevation changes. All  
30 lakes have been reported by Smith et al. (2009) but here we rename the Kamb 3 and Kamb 4 as K34 because they seem to be a single lake (Figure 5a). In early 2012, the lake K34 begins to discharge the excess water added during the preceding year. At the peak of the K34 volume increase (January 2012), K1 begins to increase in volume, strongly suggesting a linkage between the upper (K34) and lower (K1) lake (Figure 5c). The discharge of lake K1 begins in early 2013 (January 2013) and continues until the present. The timing of the discharge from the lake K1 is coincident with or slightly precedes a filling



event of KT1 (February 2013), implying that the lake K1 is supplying the water to the lakes in the KIS trunk. On the other hand, the lake K8 rapidly drains its water in the end of 2012. However, it is not clear the connection between K8 drainage and other SGLs activities in the KIS, since the pathway from lake K8 to lake K1 or lakes in the KIS trunk is still uncertain (Goeller et al., 2015). Any distinct activities are not observed in the lakes K5 and K2 downstream of lake K8 during the study period.

### 3.2 Influence of subglacial water on the Kamb Trunk estuary

The observed lake activity above indicates that subglacial melt water likely flows in a connected system from the upstream catchment area to the grounding line in the KIS. This water flux through the KIS grounding line region has a significant effect on it. We interpret a topographically low area downstream of KT3 as a kind of subglacial ‘estuary’ with hydraulic potential very close to that of the ocean at the grounding line (Figure 6a). A slight surface elevation lowering (i.e. thinning of ice) of  $\sim 0.1$  m/yr on average is seen over the estuary area downstream of KT3 using both ICESat (from 2003 to 2009) and Cryosat-2 (from 2010 to present) measurements (Figure 6b and Figure 6c). By combining ICESat and Cryosat-2 elevation time series, we find that the estuary has a three-stage elevation change pattern that indicates an acceleration in thinning after the lake activity in 2013 (Figure 6d). From 2003 to 2008, the elevation lowers at a rate of 0.1 m/yr, but the rate decreases by half (to 0.06 m/yr) between mid-2010 and early 2013 based on Cryosat-2 data. This may be associated with the cessation of KT1 drainage in this period, because the ICESat observes  $\sim 0.6$  m/yr elevation lowering in the lake KT1 from 2003 to 2008 (Smith et al., 2009) but the Cryosat-2 elevations do not show any significant elevation change before 2013 (Figure 4). Since early 2013, as subglacial lake activity increased (specifically as drainage of K1 began), the thinning rate in the estuary region increased to 0.25 m/yr. This implies that thinning in the estuary region is controlled by water flux.

We presume that a part of basal water flow from KT3 is converted to distributed basal flow such as sheet flow in the estuary, since the hydraulic potential around the estuary has a fan-shaped feature (Figure 6a) and ice-penetrating radar data near the outlet of lake KT3 shows a very flat topography (Catania et al., 2006). If the distributed basal flow exists, it increases the lubrication of ice sheet bed and decreases drag force on ice sheet flow. Tensile forces inherent between the moving ice shelf and the stagnant grounded ice can stretch and thin the ice sheet in the lubricated estuary region. Therefore, the large amount of basal water supplied by flood event might accelerate the thinning of ice sheet. This explanation is supported by the fact that the ice sheet around the estuary is not entirely stagnant, i.e. the ice flow velocity from InSAR (Rignot et al., 2011) around estuary slightly exceeds their uncertainty (Figure 1).

While a part of the inferred channel flow seems to be converted to a distributed flow pattern in the lowest part of the ice stream hydrologic system, there is some evidence that a channelized flow is still maintained in the estuary. The background MOA image in the blue rectangle of Figure 6a shows a narrow sink near the grounding line downstream of KT3. A detailed examination of Landsat images during last two decades shows the feature is continuously extending upstream (Figure 7). Considering its retreat rate ( $\sim 100$  m/yr), the length from the grounding line (8 - 9 km) and the retreat rate of grounding line ( $\sim 30$  m/yr from Thomas et al. (1988)), the feature seems to start retreating no long ( $\sim 110$  years ago) after the



stagnation of KIS. The feature is too concave for the Cryosat-2 to measure its inside elevations but the ICESat measurements represent a large elevation decrease inside the feature (up to  $\sim 1.5$  m/yr and in average  $\sim 1.2$  m/yr along 221 ICESat track) (Figure 7). We suppose that this feature was formed by a basal melting induced by the outflow of subglacial water into the sub-ice-shelf cavity. Recent studies (Alley et al., 2016; Le Brocq et al., 2013) have proposed a plausible physical mechanism to explain a line-shaped trough pattern on the ice shelf surface: they have suggested that when the subglacial melt water in grounded ice sheet flows to oceans, the heat from warmer ocean water is supplied to ice through an intermediation of subglacial water and thus dissolves the ice bottom. A similar mechanism is proposed by Marsh et al. (2016) for the WIS subglacial channel outflow area. If this mechanism is applicable to the KIS, the strong basal melting by the outflow of subglacial water can make a narrow cavity retreating upstream because the ice sheet advance toward the ice shelf is quite slow ( $\sim 7$  m/yr) in this area. Consequently, we speculate the feature is in the association with subglacial meltwater channel linked to sub-ice-shelf cavity. Since other similar features are not observed around the grounding line of KIS, it is believed that the present-day KIS trunk has a single subglacial channel that reaches the grounding line, as previous studies predicted (Carter and Fricker, 2012; Goeller et al., 2015).

#### 4 Discussion

One of the hypotheses explaining the stagnation of KIS is a conversion from sheet basal water flow to channelized flow, which causes dewatering of the subglacial deforming till and thus immobilizing it (Retzlaff and Bentley, 1993). Our observations may provide support for this hypothesis. The newly discovered subglacial lakes in the KIS trunk and distinctive elevation changes in the KIS trunk estuary suggest the existence of a persistent subglacial water flow from the upstream subglacial lakes (e.g. K1 and K34) to the grounding line. The subglacial lakes also indicate a channelized water flow since they are exactly located on a streamline inferred from the hydraulic potential map, and their sequential behaviors are probably due to open conduits, which are open and close based on subglacial lake activity, among the lakes. Considering the balance flow rate of  $\sim 6$  m<sup>3</sup>/s to the lakes in the KT trunk mentioned above, the minimum radius of a single semicircular tunnel could be approximated in the range of 1 – 2 m from an empirical relation of the discharge rate with a semi-circular cross-section and the gradient of hydraulic potential (see the supplementary method of Wingham et al. (2006b)).

Previous model predictions and observations in the upstream region of “sticky spots” in the KIS show the diversion of basal water to the neighboring WIS (Anandkrishnan and Alley, 1997; Carter and Fricker, 2012), supporting the water-piracy hypothesis for the stagnation of KIS (Alley et al., 1994). Because volume change of the upstream lakes K1 or K34 is significantly larger than that of the SGLs in the trunk of KIS, the water-piracy hypothesis might be indirectly supported. However, the connection between the upstream lakes in the KIS and the SGLs in the WIS is currently unclear from our observations. Our results only confirm the subglacial water system in the bigger and faster WIS is more active than the KIS trunk subglacial lake system, since volume changes in the WIS system are apparently 3 - 10 times as large as in the KIS trunk system (Siegfried et al., 2016). Marsh et al. (2016) reported extremely large melt rates ( $22.2 \pm 0.2$  m/yr) where



subglacial water discharge is expected on Mercer/Whillans Ice Stream grounding line . A strong basal melt is also inferred from the elevation lowering (up to ~ 1.5 m/yr) in the narrow channel near the grounding line of KIS, but the basal melt rate cannot be exactly projected from the observed elevation lowering due to the ambiguity of floating equilibrium on the narrow channel. However, the basal melt rate might be smaller than those on Mercer/Whillans Ice Stream, because the narrow  
5 channel near the grounding line is not likely to be freely floating on seawater. At present, our results can not definitely prove which of the basal water channelization hypothesis or the water-piracy hypothesis is suitable for the stagnation of KIS. Further studies on the basal flow channel in the KIS trunk are necessary to fix this puzzling.

*Acknowledgements.* This work was supported by a Korea Polar Research Institute (KOPRI) project (Grant No. PM15020)  
10 funded by the Ministry of Oceans and Fisheries, Korea and national research foundation grant NRF2013R1A1A2008368. The Cryosat-2, ICESat, and Landsat data used in this study are available from the European Space Agency, the National Snow and Ice Data Center, the U.S. Geological Survey respectively.

## References

- 15 Alley, K. E., Scambos, T. A., Siegfried, M. R., and Fricker, H. A.: Impacts of warm water on Antarctic ice shelf stability through basal channel formation, *Nat. Geosci.*, 9, 290-293, 2016.
- Alley, R. B., Anandakrishnan, S., Bentley, C. R., and Lord, N.: A water-piracy hypothesis for the stagnation of Ice Stream C, *Antarctica, Ann. Glaciol.*, 20, 187-194, 1994.
- 20 Anandakrishnan, S. and Alley, R. B.: Stagnation of ice stream C, West Antarctica by water piracy, *Geophys. Res. Lett.*, 24, 265-268, 1997.
- Bell, R. E.: The role of subglacial water in ice-sheet mass balance, *Nat. Geosci.*, 1, 297-304, 2008.
- Carter, S. P., Blankenship, D. D., Young, D. A., Peters, M. E., Holt, J. W., and Siegert, M. J.: Dynamic distributed drainage implied by the flow evolution of the 1996-1998 Adventure Trench subglacial lake discharge, *Earth Planet. Sc. Lett.*, 283, 24-37, 2009.
- 25 Carter, S. P. and Fricker, H. A.: The supply of subglacial meltwater to the grounding line of the Siple Coast, West Antarctica, *Ann. Glaciol.*, 53, 267-280, 2012.
- Catania, G., Hulbe, C., Conway, H., Scambos, T. A., and Raymond, C. F.: Variability in the mass flux of the Ross ice streams, West Antarctica, over the last millennium, *J. Glaciol.*, 58, 741-752, 2012.
- Catania, G., Scambos, T. A., Conway, H., and Raymond, C. F.: Sequential stagnation of Kamb Ice Stream, West Antarctica, *Geophys. Res. Lett.*, 33, 2006.
- 30 Fretwell, P., Pritchard, H. D., Vaughan, D. G., Bamber, J. L., Barrand, N. E., Bell, R., Bianchi, C., Bingham, R. G., Blankenship, D. D., Casassa, G., Catania, G., Callens, D., Conway, H., Cook, A. J., Corr, H. F. J., Damaske, D., Damm, V., Ferraccioli, F., Forsberg, R., Fujita, S., Gim, Y., Gogineni, P., Griggs, J. A., Hindmarsh, R. C. A., Holmlund, P., Holt, J. W., Jacobel, R. W., Jenkins, A., Jokat, W., Jordan, T., King, E. C., Kohler, J., Krabill, W., Riger-Kusk, M., Langley, K. A., Leitchenkov, G., Leuschen, C., Luyendyk, B. P., Matsuoka, K., Mouginot, J., Nitsche, F. O., Nogi, Y., Nost, O. A., Popov, S. V., Rignot, E., Rippin, D. M., Rivera, A., Roberts, J., Ross, N., Siegert, M. J., Smith, A. M., Steinhage, D., Studinger, M., Sun, B., Tinto, B. K., Welch, B. C., Wilson, D., Young, D. A., Xiangbin, C., and Zirizzotti, A.: Bedmap2: improved ice bed, surface and thickness datasets for Antarctica, *Cryosphere*, 7, 375-393, 2013.
- 40 Fricker, H. A. and Scambos, T.: Connected subglacial lake activity on lower Mercer and Whillans Ice Streams, West Antarctica, 2003-2008, *J. Glaciol.*, 55, 303-315, 2009.



- Fricker, H. A., Scambos, T., Bindschadler, R., and Padman, L.: An active subglacial water system in West Antarctica mapped from space, *Science*, 315, 1544-1548, 2007.
- Fried, M. J., Hulbe, C. L., and Fahnestock, M. A.: Grounding-line dynamics and margin lakes, *Ann. Glaciol.*, 55, 87-96, 2014.
- 5 Goeller, S., Helm, V., Thoma, M., and Grosfeld, K.: Subglacial hydrology indicates a major shift in dynamics of the West Antarctic Ross Ice Streams within the next two centuries, *Cryosphere*, 9, 3995-4018, 2015.
- Goovaert, P.: *Geostatistics for Natural Resources Evaluation*, Oxford, New York, 1997.
- Gray, L.: Evidence for subglacial water transport in the West Antarctic Ice Sheet through three-dimensional satellite radar interferometry, *Geophys. Res. Lett.*, 32, 2005.
- 10 Helm, V., Humbert, A., and Miller, H.: Elevation and elevation change of Greenland and Antarctica derived from CryoSat-2, *Cryosphere*, 8, 1539-1559, 2014.
- Hulbe, C. and Fahnestock, M.: Century-scale discharge stagnation and reactivation of the Ross ice streams, West Antarctica, *J. Geophys. Res.-Earth Surface*, 112, 2007.
- Le Brocq, A. M., Ross, N., Griggs, J. A., Bingham, R. G., Corr, H. F. J., Ferraccioli, F., Jenkins, A., Jordan, T. A., Payne, A. J., Rippin, D. M., and Siegert, M. J.: Evidence from ice shelves for channelized meltwater flow beneath the Antarctic Ice Sheet, *Nat. Geosci.*, 6, 945-948, 2013.
- Livingstone, S. J., Clark, C. D., Woodward, J., and Kingslake, J.: Potential subglacial lake locations and meltwater drainage pathways beneath the Antarctic and Greenland ice sheets, *Cryosphere*, 7, 1721-1740, 2013.
- 20 Marsh, O. J., Fricker, H. A., Siegfried, M. R., Christianson, K., Nicholls, K. W., Corr, H. F. J., and Catania, G.: High basal melting forming a channel at the grounding line of Ross Ice Shelf, Antarctica, *Geophys. Res. Lett.*, 43, 250-255, 2016.
- McMillan, M., Shepherd, A., Sundal, A., Briggs, K., Muir, A., Ridout, A., Hogg, A., and Wingham, D.: Increased ice losses from Antarctica detected by CryoSat-2, *Geophys. Res. Lett.*, 41, 3899-3905, 2014.
- Pritchard, H. D., Arthern, R. J., Vaughan, D. G., and Edwards, L. A.: Extensive dynamic thinning on the margins of the Greenland and Antarctic ice sheets, *Nature*, 461, 971-975, 2009.
- 25 Retzlaff, R. and Bentley, C. R.: Timing of stagnation of ice stream C, West Antarctica from short-pulse-radar studies of buried surface crevasses, *J. Glaciol.*, 39, 553-561, 1993.
- Rignot, E., Mouginot, J., and Scheuchl, B.: Ice flow of the Antarctic ice sheet, *Science*, 333, 1427-1430, 2011.
- Siegfried, M. R., Fricker, H. A., Carter, S. P., and Tulaczyk, S.: Episodic ice velocity fluctuations triggered by a subglacial flood in West Antarctica, *Geophys. Res. Lett.*, doi: 10.1002/2016gl067758, 2016.
- 30 Smith, B. E., Fricker, H. A., Joughin, I. R., and Tulaczyk, S.: An inventory of active subglacial lakes in Antarctica detected by ICESat (2003-2008), *J. Glaciol.*, 55, 573-595, 2009.
- Thomas, R. H., Stephenson, S. N., Bindschadler, R. A., S., S., and Bentley, C. R.: Thinning and Grounding-line Retreat on Ross Ice Shelf, Antarctica, *Ann. Glaciol.*, 11, 165-172, 1988.
- 35 van der Wel, N., Christoffersen, P., and Bougamont, M.: The influence of subglacial hydrology on the flow of Kamb Ice Stream, West Antarctica, *J. Geophys. Res.-Earth Surface*, 118, 97-110, 2013.
- Wang, F., Bamber, J. L., and Cheng, X.: Accuracy and Performance of CryoSat-2 SARIn Mode Data Over Antarctica, *IEEE Geosci. Remote S.*, 12, 1516-1520, 2015.
- 40 Wingham, D. J., Francis, C. R., Baker, S., Bouzinac, C., Brockley, D., Cullen, R., de Chateau-Thierry, P., Laxon, S. W., Mallow, U., Mavrocordatos, C., Phalippou, L., Ratier, G., Rey, L., Rostan, F., Viau, P., and Wallis, D. W.: CryoSat: A mission to determine the fluctuations in Earth's land and marine ice fields, *Adv Space Res-Series*, 37, 841-871, 2006a.
- Wingham, D. J., Siegert, M. J., Shepherd, A., and Muir, A. S.: Rapid discharge connects Antarctic subglacial lakes, *Nature*, 440, 1033-1036, 2006b.

45



5

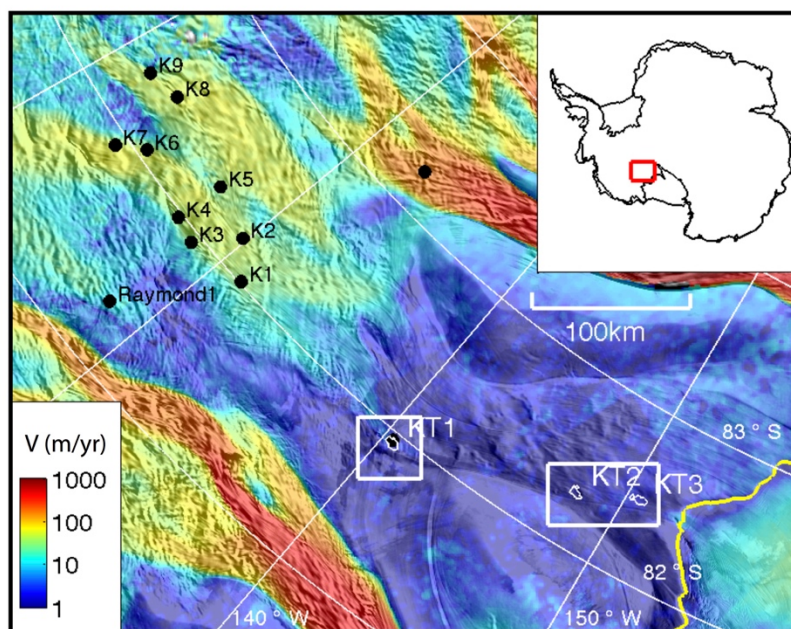
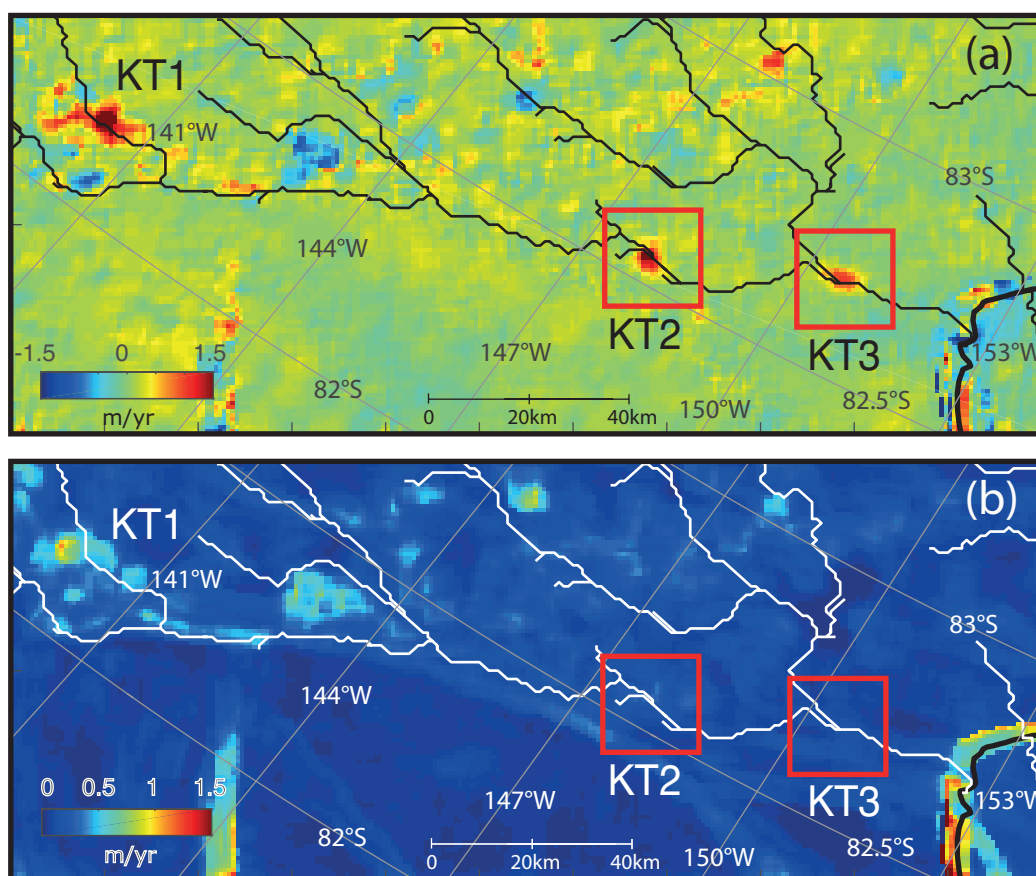


**Figure 1:** Locations of subglacial lakes in the KIS glacial catchments including the newly identified lakes KT2 and KT3 in the trunk of KIS. The color shading shows the InSAR-based ice velocity from MEaSURES on the MOA image. The white rectangles indicate the areas shown in Fig. 3.

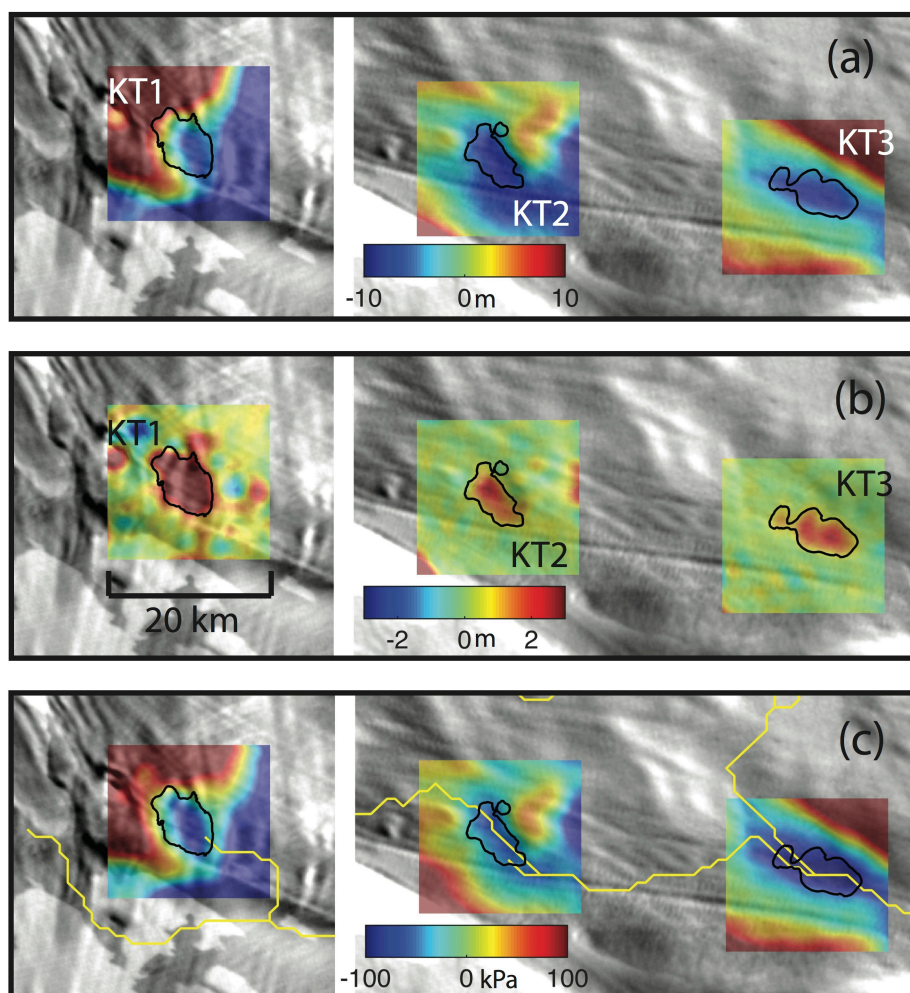
10



5



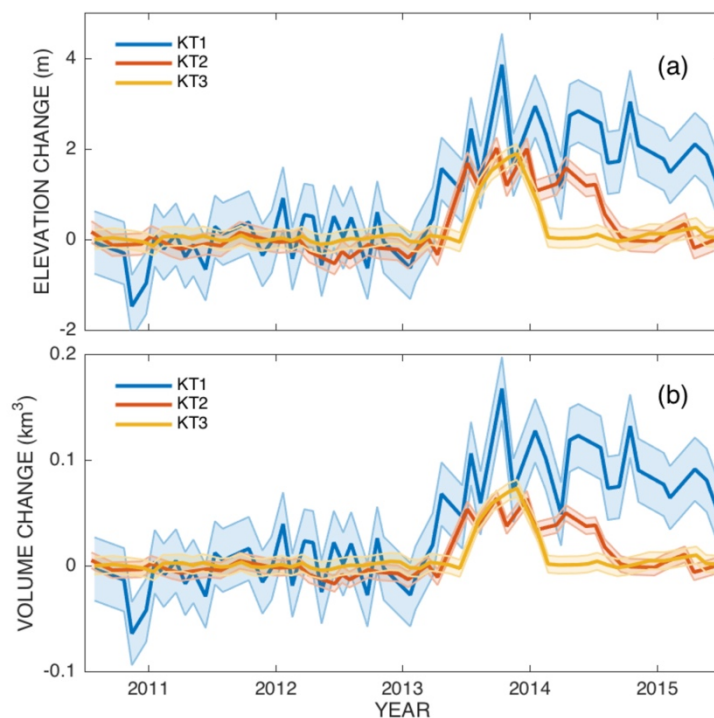
10 **Figure 2: (a) Elevation change rates and (b) their uncertainties (95% confidence interval) around the trunk of KIS for two years (February 2012 - January 2014). The polylines present the subglacial streamlines extracted from the hydraulic potential. The red boxes indicate the location of lakes KT2 and KT3.**



5 **Figure 3:** Ice surface elevations and elevation anomalies around the subglacial lakes overlaid on the MOA image. (a) Reference DEM (color shading) derived by the kriging method using the Cryosat-2 elevation measurements. Note that the mean elevation values in each rectangular area are subtracted in order to reveal the details. (b) Elevation anomaly deviated from the reference DEM in the time windows as mentioned in the text. (c) Hydraulic potential calculated using the reference DEM and ice thickness from Bedmap2. The yellow lines indicate the subglacial streamlines inferred from the hydraulic potential.



5

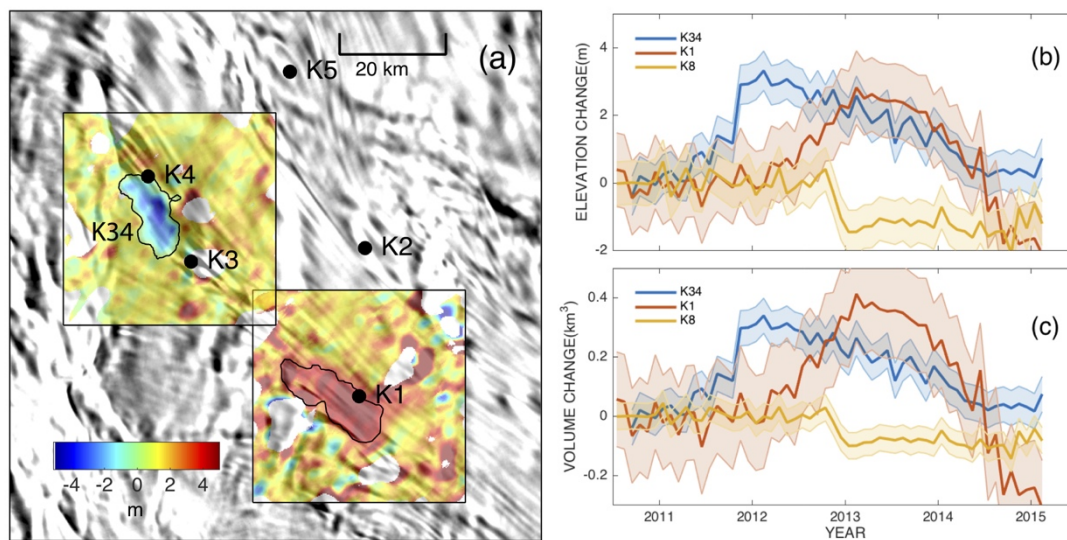


10 **Figure 4: Temporal (a) elevation and (b) volume changes of subglacial lakes in the trunk of KIS. The error range displayed by transparent color is empirically determined as the standard deviation of elevation measurements on the stationary ice adjacent to each lake.**

15



5



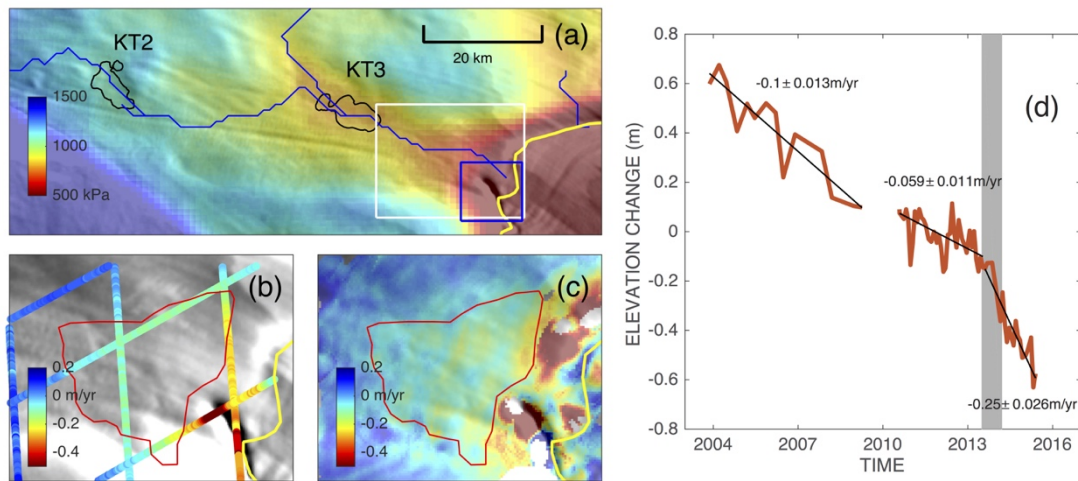
10

**Figure 5: Spatial and temporal changes of the subglacial lakes in the upper region of KIS. (a) DEM difference (color shading) around the subglacial lakes K1 (2013 – 2011) and K34 (2014 – 2012). The difference in the area with large kriging uncertainties (>90%) is masked. The polygons indicate the lake boundaries. The black dots are the locations of the lakes already listed in Wright and Siegert [2012]. The right panels show the temporal (b) elevation and (c) volume changes of lakes.**

15



5



10 **Figure 6: Elevation changes near the KIS grounding line. (a) Hydraulic potential (color shading) and flow lines (blue line) from**  
**KT2 to the grounding line (yellow line). The white rectangle indicates the area displayed in (b) and (c). The blue rectangle indicate**  
**the area shown in Figure 7. (b) Elevation change rate estimated from ICESat repeat track analysis. (c) Elevation change rate**  
**estimated from Cryosat-2 DEM differencing (2014-2011). (d) Temporal elevation changes of ICESat and Cryosat-2 measurments**  
**in the ‘estuary’ area denoted by the red polygon in (b) and (c). The bias of Cryosat-2 elevations was removed, including the**  
 15 **instrument bias (0.67 m) and the effect of radar penetration into the snow pack (1.03m) which is estimated along an adjacent**  
**ICESat track. The gray rectangle indicates the entire fill-drain event of lake KT3.**



5

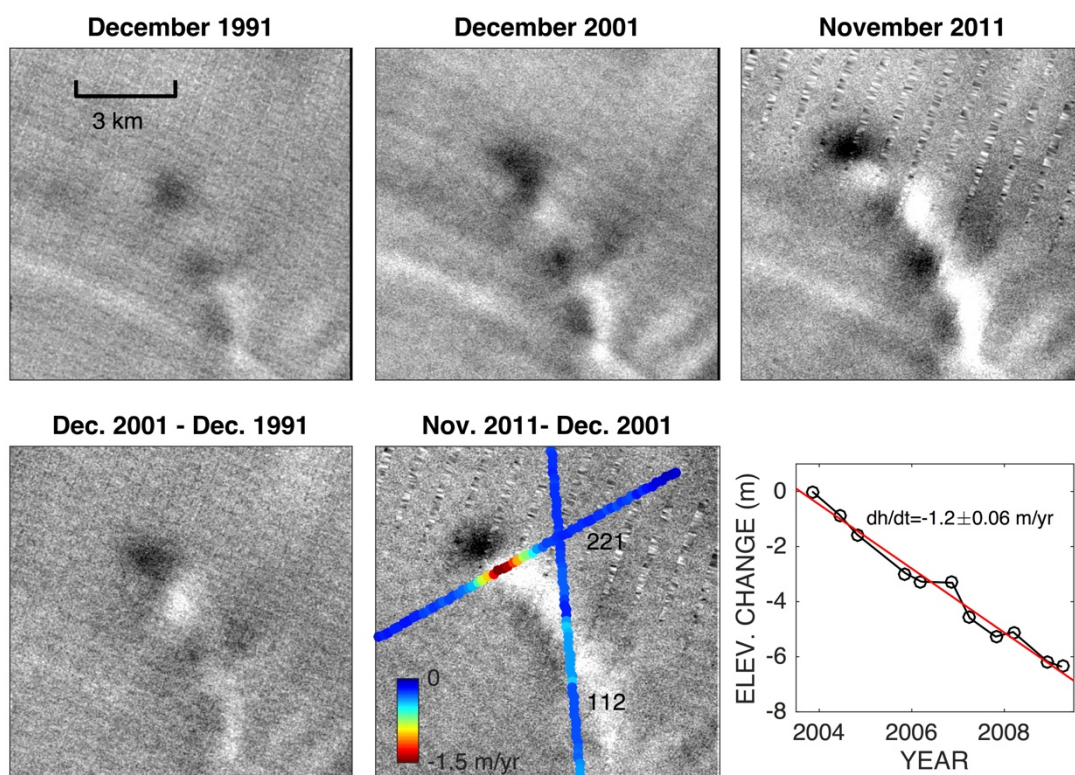


Figure 7: Landsat images (upper) and their difference images (lower) over the region indicated by the blue box in Figure 6. The stripes in the image in November 2011 due to the failure of the scan line corrector (SLC) of Landsat-7 ETM+ are removed by a gap filling method using additional images around the same time. The elevation change rates from the ICESat measurements are overlaid on the difference image (lower middle panel). The lower right panel shows the temporal elevation change in the topographic sink measured along the 221 ICESat track.

10

15